MEDICAL SCIENCE MONITOR

MEDICAL TECHNOLOGY

e-ISSN 1643-3750
© Med Sci Monit, 2018; 24: 2003-2017
DOI: 10.12659/MSM.906903

Received: 2017.08.30
Accepted: 2017.09.14
Published: 2018.04.05

The Effects of Left Ventricular Assist Device Support Level on the Biomechanical States of Aortic Valve

Authors' Contribution:
Study Design A
Data Collection B
Statistical Analysis C
Data Interpretation D
Manuscript Preparation E
Literature Search F
Funds Collection G

BEF Qi Zhang
CDEFG Bin Gao
G Chang Yu

School of Life Science and BioEngineering, Beijing University of Technology, Beijing, P.R. China

Corresponding Author: Bin Gao, e-mail: gaobin@bjut.edu.cn
Source of support: Publication charges for this article have been funded by the National Natural Science Foundation of China (Grant No. 11602007, 91430215, 11572014, 11272022,), and BJUT Foundation Fund (Grant No.015000514316007)

Background: Although aortic valve disease caused by left ventricular assist device (LVAD) support has attracted more and more attention, the precise biomechanical effects of LVAD support level on the aortic valve are still unclear.

Material/Methods: A structural finite element models study was conducted using an ideal aortic valve geometric model. Four different study conditions were designed, according to the reduction of the open duration of the aortic valve. The isotropic hyperelastic constitutive equation was chosen to reflect the mechanical property of the leaflets. The distribution of the stress, strain, and transient dynamics of the leaflet were calculated.

Results: Along with the increase of LVAD support level, the open duration of the aortic valve was also reduced by the increase of LVAD support (low support level case 0.23 seconds versus middle support level case 0.2 seconds versus high support level case 0.14 seconds). Moreover, along with the increase of support mode of LVAD, the von Mises stress in most leaflet areas was increased from the low stress level (0–0.4 MPa) to the middle region (0.4–0.8 MPa). Once the leaflets were continuously closed, the high stress level (larger than 0.8 MPa) was observed. In contrast, the support level of LVAD only had slight effects on the distribution of von Mises strain. According to the aforementioned results, maintaining the open duration of aortic valve longer than 0.2 seconds could achieve better performance of biomechanical states of leaflets.

Conclusions: This study could provide useful information on the determination of optimal LVAD support strategy.

MeSH Keywords: Aortic Valve • Biomechanical Phenomena • Finite Element Analysis

Full-text PDF: https://www.medscimonit.com/abstract/index/idArt/906903

Indexed in: [Current Contents/Clinical Medicine] [SCI Expanded] [ISI Alerting System] [ISI Journals Master List] [Index Medicus/MEDLINE] [EMBASE/Excerpta Medica] [Chemical Abstracts/CAS]

Background

With the prevalence heart failure increasing, it has become a severe threat to human health [1]. The left ventricular assist device (LVAD) has become an important method for heart failure patients to improve quality of life and prolong survival [2]. Along with the wide use of LVAD, the impairment of the aortic valve's structure and function has attracted more and more attention. For instance, Connelly et al. reported that more than 60% of patients supported by LVAD suffered from commissural fusion of the aortic valve [3]. Similarly, Banchs et al. reported that the patients supported by LVAD had a higher prevalence of acquired aortic cusp fusion [4]. Besides that, aortic insufficiency was confirmed as another complications caused by LVAD support. Hata et al. demonstrated that after LVAD support, more than 50% of patients suffered from aortic insufficiency, 48.6% of patients suffered from partial aortic valve fusion, and curling with leaflet shortening was detected in 62.9% of patients [5].

The LVAD, including the axial flow pump and centrifugal pump, usually bypasses the native heart. The outflow cannula of LVAD usually is anastomosed at the ascending aorta, and the inlet flow cannula of LVAD is anastomosed at the left ventricle. The blood is pumped by the LVAD from the left ventricle to the ascending aorta. That means that the aortic pressure increases along with increased support level of LVAD, while the left ventricular pressure is gradually reduced. These changes in biomechanical environment are considered important, resulting in aortic valve diseases. It has been demonstrated that aortic valve degradation is an active process, involving perturbation of valvular endothelial cells and interstitial cells by the local mechanical forces [6,7]. A previous study that examined the effects of pressure on aortic leaflets demonstrated that increases in pressure decreased the α-smooth muscle actin (α-SMA) expression [8]. Similarly, Warnock et al. investigated the immediate response of elevated pressure on valve interstitial cells and found significant upregulation of vascular cell adhesion molecule-1 (VCAM-1) and downregulation of osteopontin [9]. In addition, the collagen content of the aortic value leaflets, stretched to pathological levels for 48 hours, was increased when compared to fresh and static control leaflets [10]. Hence, we hypothesized that the changes in biomechanical environment, caused by LVAD support, is an important reason for aortic valve degradation. However, the precise effect of LVAD support on the biomechanical environment of the aortic valve is still unclear.

Currently, structural finite element models (FEMs) are widely used to study the biomechanical environment of the aortic valve. For instance Marom et al. utilized the FEMs method to determine the influence of aortic annulus diameter on aortic valve mechanics [11]. Auricchio et al. studied the stress distribution of transcatheter aortic valve in a patient-specific model by using the FEMs approach [12]. Similarly, Labrosse et al. proposed a novel FEM of the natural aortic valve, with anisotropic hyperelastic material properties for the leaflets [13]. The aforementioned studies demonstrated that FEMs approach could provide useful information on the aortic valve biomechanics.

In our present study, the changes in biomechanics of the aortic valve under LVAD support were studied using the FEMs approach. Ideal structural FEM of the aortic valve was established. Four support levels, named as low support level case, middle support level case, high support level case, and full support level case, were chosen as the study conditions. All support levels were classified according to the reduction of the open duration of the aortic valve. In addition, a "healthy condition" was used as the control group. All of the five study conditions were obtained from a validated lumped parameter model of the cardiovascular system with LVAD support [14]. The isotropic hyperelastic constitutive equation was chosen to reflect the mechanical property of the leaflets. The distribution of the stress, the distribution of the strain, and the transient dynamics of the leaflet were calculated to evaluate the changes in aortic valve biomechanics.

Material and Methods

A structural finite element model (FEM) of ideal aortic valve was established. The dynamic simulations were conducted by using the commercial explicit finite element solver LS-DYNA 971 Release 7 (LSTC, Livermore, CA, USA). The geometric model was discretized by using Gambit (ANSYS, Inc.). The time step was set to 2us to maintain the accuracy of results. And three cardiac cycles were calculated to eliminate the influence of the initial condition. The results, calculated at the third cardiac cycle, were extracted for evaluating the motion and biomechanical states of aortic valve. The simulation was performed on Intel Xeon (2.93 GHz) workstation with 16 processors and required 28 hours for computation.

Aortic valve geometrical model and discretization

The aortic valve geometrical model was constructed, including ascending aorta, three leaflets, aortic root, and the sinus of Valsalva (Figure 1A, 1B), in which the geometric size was the same as reported in the literature [15]. In this model, the aortic valve leaflets were discretized into 28,760 tetrahedral elements, while the other parts of the model were meshed by 131,959 8-nodes hexahedral elements with a single integration point, which could reduce the computational cost (Figure 1C, 1D). The number of element was determined according to the results of the grid independent test.

Indexed in: [Current Contents/Clinical Medicine] [SCI Expanded] [ISI Alerting System] [ISI Journals Master List] [Index Medicus/MEDLINE] [EMBASE/Excerpta Medica] [Chemical Abstracts/CAS]

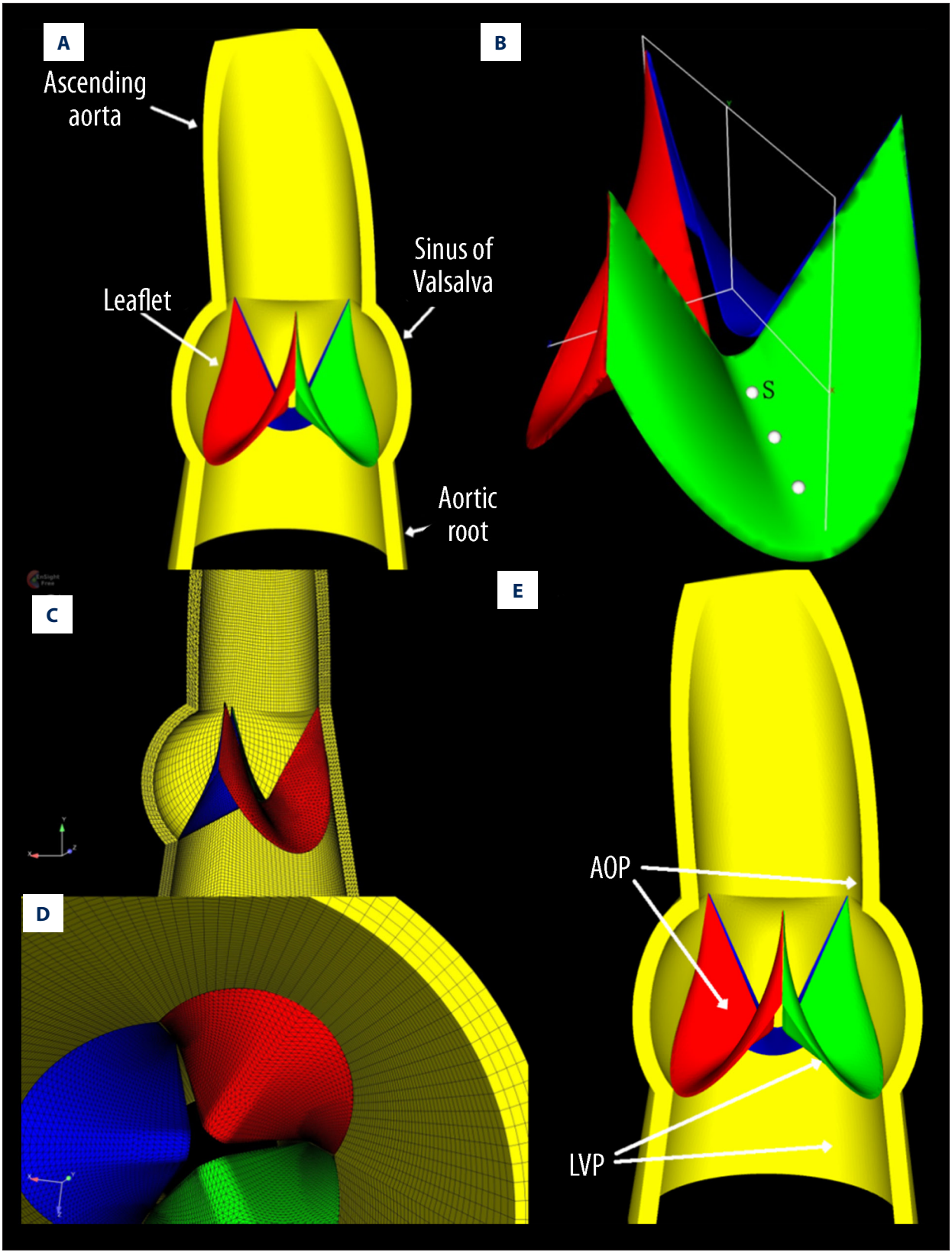

Figure 1. The geometric model of aortic valve. (**A, B**) The anatomical structure of the aortic valve model. (**C, D**) The mesh and grid type of the finite element model of the aortic valve. (**E**) The type and position of the boundary condition, employed in this study.

Indexed in: [Current Contents/Clinical Medicine] [SCI Expanded] [ISI Alerting System] [ISI Journals Master List] [Index Medicus/MEDLINE] [EMBASE/Excerpta Medica] [Chemical Abstracts/CAS]

Table 1. Mooney-Rivlin material parameters for porcine leaflet properties.

Parameters	C_{10}	C_{10}
Values (kPa)	33	2.9

Constitutive models

The density was set as 1,100 kg/m^3 for all the parts of the aortic valve model [16]. In this study, the mechanical property of the aortic valve leaflets was modeled as nearly incompressible, hyperelastic, and isotropic material. And the invariant-based strain energy function, named as "MAT_027", was adopted [17]. The strain energy function is a two-parametric Mooney-Rivlin hyperelastic model, which is defined as the equation:

$$W=C_{10}(I_1-3)+C_{01}(I_2-3)+A(I_3^{-2}-1)+D(I_3-1)^2 \quad (1)$$

Where I_1 and I_2 are the principal invariants of the Cauchy-Green deformation tensor. As the leaflet was assumed as incompressible material, I_3=1. Hence, the parameters A and D is neglected for this study. The C_{10} and C_{01} are the material parameters, which are set according to the Cao and Sucosky study [18]. The values of material property of aortic valve leaflets are listed in Table 1.

The other parts of the aortic valve were modeled as linear elastic and isotropic material, in which the Poisson's ratio was set as 0.3 and the Young's modulus was 2 MPa [19].

The boundary conditions

The model of aortic valve was firstly pressurization to 80 mm Hg to achieve an initial state for all cases. Then two complete cardiac cycles were simulated by applying the pulsatile aortic (AOP) and ventricular (LVP) pressures, which were obtained from *in vitro* LVAD experiments. The pressure load was applied as a uniformly distributed surface load. AOP was applied on the ascending aortic inner wall and the surface of aortic valve leaflets, aiming to the ascending aorta. Similarly, LVP was applied on the aortic root's inner wall and the surface of the aortic valve leaflets, aiming to the left ventricle (Figure 1E).

In this work, LVAD was bypassed with the native heart, according to the clinical practice. Four support levels of LVAD, named as low support level case, middle support level, high support level case, and full support level case, were designed according to the reduction of the open duration of the aortic valve. And the healthy condition was chosen as the control group. A lumped parameter model of cardiovascular system with LVAD support, which accuracy was validated by clinical data, was utilized to generate the boundary conditions [14] (Figure 2A). Along with the increase of support level of LVAD, the open duration of the aortic valve was reduced, and the waveforms of the left ventricular pressure (LVP) and aortic pressure (AOP) were derived (Figure 2B–2F).

Time integration algorithm

LS-DYNA uses the central difference method, which gives a second order accurate integration, to advance the position of the Lagrangian mesh in time. For every time step Δt, algorithm iterates the following steps.

First, the values of displacement and velocity of nodes were updated as the equation:

$$\mu_{n+1}=\mu_n+\Delta t_{n+\frac{1}{2}}\cdot v_{n+\frac{1}{2}} \quad (2)$$

$$v_{n+1}=v_{n-\frac{1}{2}}+\Delta t\cdot\alpha_n \quad (3)$$

Where α_n is the acceleration of the nodes at nth time step.

And then, the internal force was calculated as the equation:

$$\varepsilon^{n+\frac{1}{2}}=B\cdot v^{n+\frac{1}{2}} \quad (4)$$

$$\sigma^{n+\frac{1}{2}}=F(\varepsilon^{n+\frac{1}{2}}) \quad (5)$$

$$\sigma^{n+\frac{1}{2}}=\sigma^n+\Delta t\sigma^{n+\frac{1}{2}} \quad (6)$$

$$f_{int}^{n+\frac{1}{2}}=\int_v B^T\sigma^{n+1}dV \quad (7)$$

Where is the internal force, B represents the strain-displacement matrix, F(ε) denotes the function of strain, depending on the material property, V is the volume of the element, ε denotes the strain of the element, and σ represents the stress of the material.

Subsequently, the external force f_{ext} was calculated by using the boundary condition and body load, and then, the acceleration was determined by summing the internal force, external force and the mass of each element, as the equation

$$\alpha^{n+1}=\frac{f_{ext}^{n+1}-f_{int}^{n+1}-cv^{n+\frac{1}{2}}}{m} \quad (8)$$

Where m denotes the mass of each element. After the acceleration was calculated, the new procedure was iterated.

Indexed in: [Current Contents/Clinical Medicine] [SCI Expanded] [ISI Alerting System] [ISI Journals Master List] [Index Medicus/MEDLINE] [EMBASE/Excerpta Medica] [Chemical Abstracts/CAS]

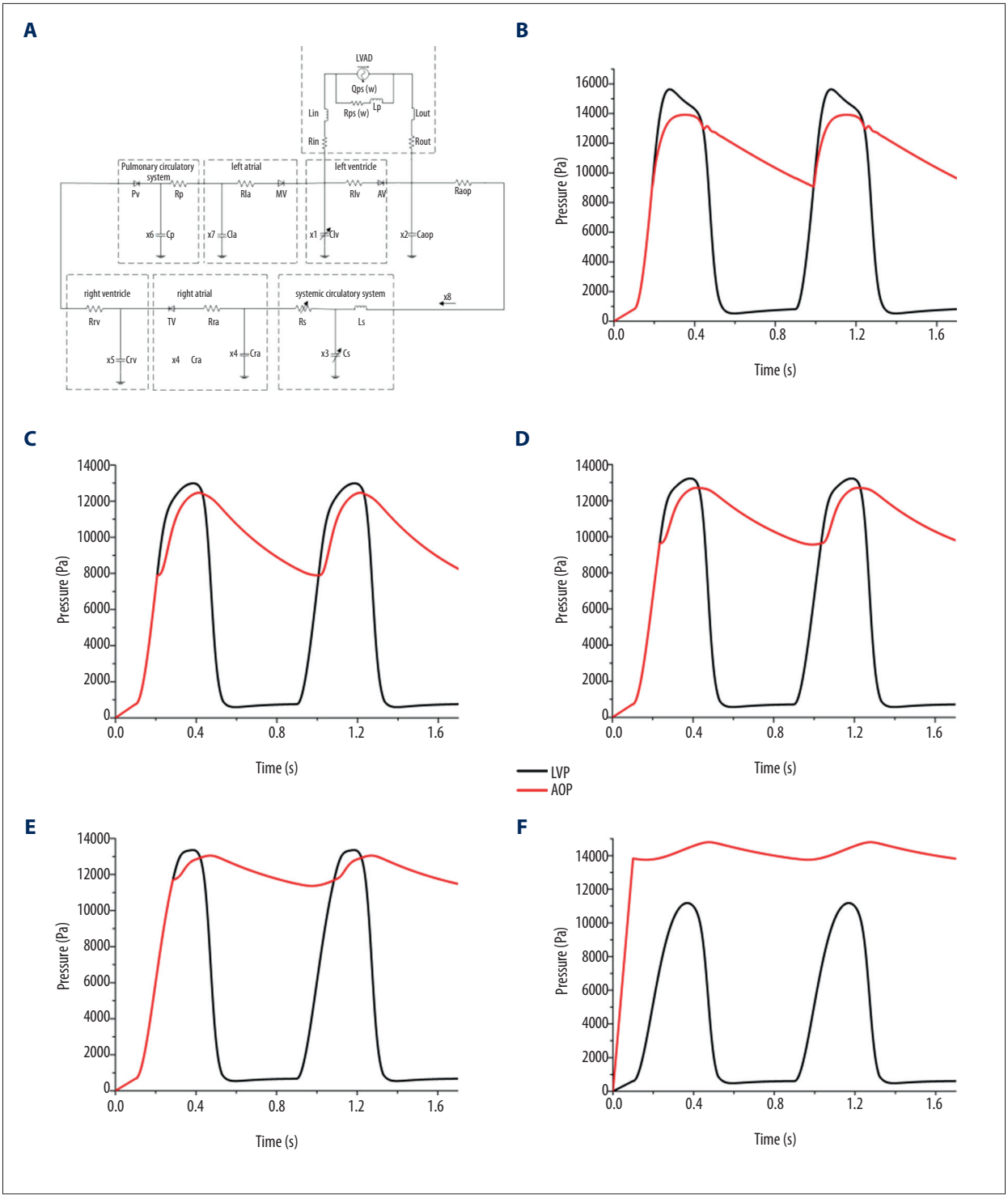

Figure 2. Loading time-dependent boundary conditions. (**A**) The lamped parameter model of cardiovascular system with LVAD support. (**B**) The pressure boundary condition, obtained from healthy condition. (**C**) The pressure boundary condition, obtained from low support level case. (**D**) The boundary condition, derived from middle support level case. (**E**) The boundary condition obtained from high support level. (**F**) The boundary condition from full support level.

Indexed in: [Current Contents/Clinical Medicine] [SCI Expanded] [ISI Alerting System] [ISI Journals Master List] [Index Medicus/MEDLINE] [EMBASE/Excerpta Medica] [Chemical Abstracts/CAS]

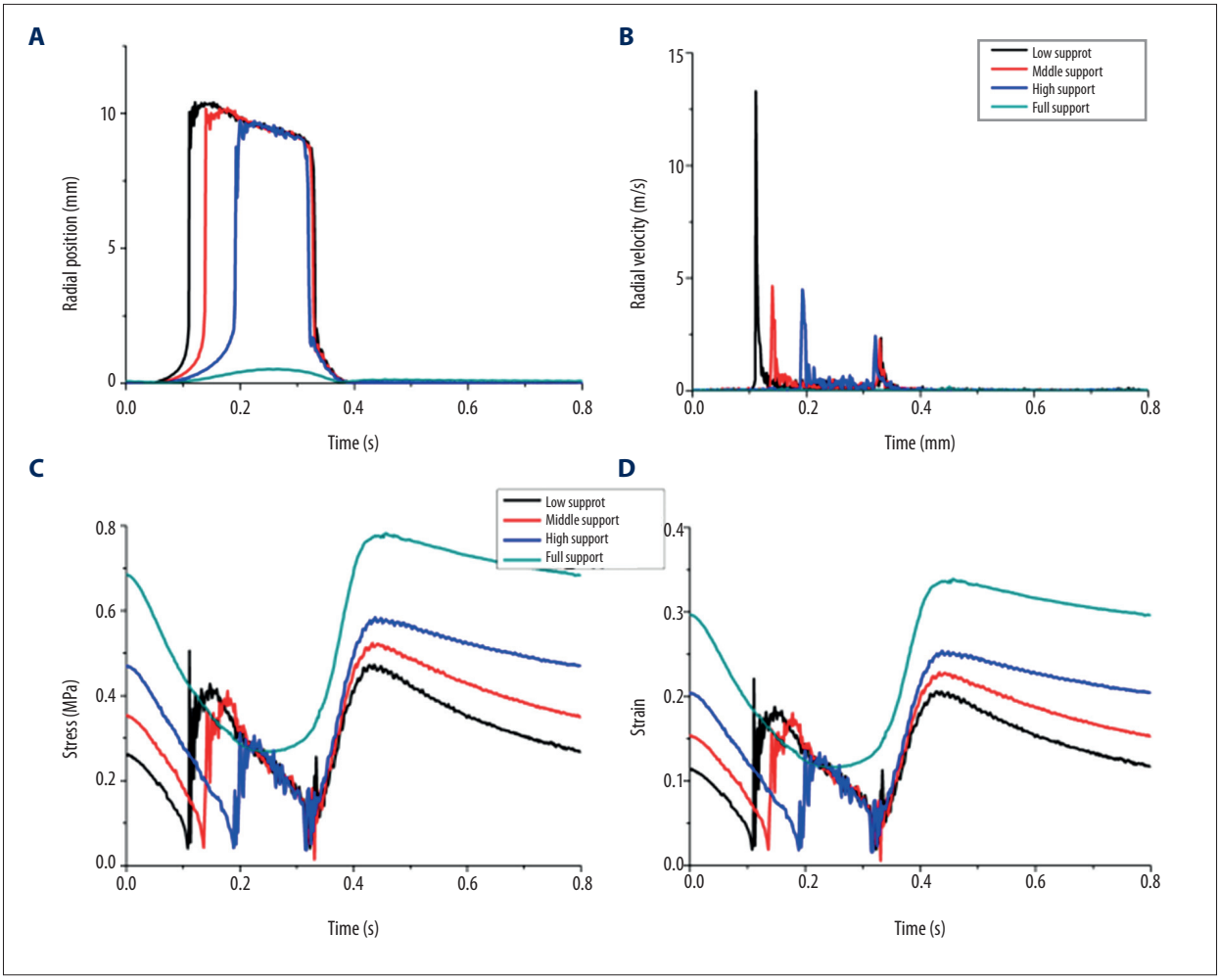

Figure 3. The transient dynamics of aortic valve. (**A**) The time-dependent radial position of the nodulus of Arantius. (**B**) The time-dependent radial velocity of the nodulus of Arantius. (**C**) The time-dependent stress of the nodulus of Arantius. (**D**) The time-dependent strain of the nodulus of Arantius.

Mechanical characterization

In this study, the global biomechanical states of aortic valve were investigated in terms of the equivalent von Mises strain and von Mises stress, which describe the overall 3D distribution of the strain ε and the stress σ of the aortic valve, which were denoted as the equations:

$$\varepsilon=\frac{\sqrt{2}}{3}[(\varepsilon_1-\varepsilon_2)^2+(\varepsilon_2-\varepsilon_3)^2+(\varepsilon_3-\varepsilon_1)^2]^{1/2} \quad (9)$$

$$\sigma=\frac{\sqrt{2}}{3}[(\sigma_1-\sigma_2)^2+(\sigma_2-\sigma_3)^2+(\sigma_3-\sigma_1)^2]^{1/2} \quad (10)$$

Where ε_1 represents the principal strain, and σ_1 denotes the principal stress. Besides that, the radial position and velocity of the leaflet was extracted for comparing the differences of the transient dynamics of aortic valve leaflet under various LVAD support levels.

Biomechanical analysis

In order to evaluate the biomechanical differences between each support levels, the time-average von Mises stress and von Mises strain were calculated according to the equation and

$$\text{TAStress}=\frac{1}{T}\int_0^T stress(t)dt \quad (11)$$

$$\text{TAStress}=\frac{1}{T}\int_0^T strain(t)dt \quad (12)$$

Where stress(t) and strain(t) represented the instantaneous value of von Mises stress and von Mises strain during the whole cardiac cycle, respectively. T denoted the cardiac cycle, which was set to be 0.8 seconds in this study.

Indexed in: [Current Contents/Clinical Medicine] [SCI Expanded] [ISI Alerting System] [ISI Journals Master List] [Index Medicus/MEDLINE] [EMBASE/Excerpta Medica] [Chemical Abstracts/CAS]

Results

The aortic valve kinematics

The aortic valve kinematics was evaluated in terms of aortic valve opening and closure dynamics during the cardiac cycle and the mechanical response to the changes in the pressure differences under different cases.

Aortic valve motion, during the cardiac cycle, was illustrated through the time-dependent radial position (Figure 3A) and radial velocity (Figure 3B) of the nodulus of Arantius (the middle point (point s) of the leaflet, Figure 1B). From Figure 3, the changes in the motion of aortic valve leaflet were obviously observed. As the aortic valve, under the full support level case, was closed throughout the whole cardiac cycle, the motion of aortic valve, under full support level, was not evaluated in this study. It is seen that along with the increase of the support level of LVAD, the time point, when the leaflet begin to rapidly open, was gradually delayed (low support level case 0.1 second versus middle support level case 0.13 second versus high support level 0.19 second) (Figure 3A). And the maxima of radial position of the leaflet were declined with the increase of LVAD support level. In order to more quantitatively evaluate the aortic valve motion, the time-dependent absolute value of the radial velocity of the noduli of Arantius [19], as a new indicator, was calculated (Figure 3B). The local maxima in the opening and closing phase were considered as the rapid valve opening (RVOT) and closure (RVCT) time, and the interval between RVOT and RVCT is the open duration of aortic valve. Although the RVOT was gradually delayed along with the increase of LVAD support level, the RVCT under the three case scenarios was nearly the same with each other. Hence the open duration of aortic valve was reduced along with the increase of LVAD support level, which is consistent with the clinical observations (low support level case 0.23 seconds versus middle support level case 0.2 seconds versus high support level case 0.14 seconds). In addition, the velocity of RVOT, under the low support level case, was significantly higher than that under other cases (low support level case 13 m/seconds versus middle support level case 4.9 m/seconds versus high support level 4.8 m/seconds).

The distribution of stress and strain

The time-dependent stress and strain of the aortic valve leaflet, under all cases were similar with each other (Figure 4C, 4D). During systolic phase, the stress and strain of the nodulus of Arantius first reduced and then begin to increase at RVOT (stress: low support level case 0.42 MPa versus middle support level case 0.38 MPa versus high support level case 0.3 MPa; strain: low support level case 0.18 versus middle support level case 0.16 versus high support level case 0.14). The results were consistent with the Cao and Sucosky study [18]. Moreover, some relative differences were also noticed in the temporal trend of systolic stress and strain of the nodulus of Arantius. The time of the maximal stress was delayed along with the increase of LVAD support level (low support level case 0.1 second versus middle support level case 0.13 second versus high support level 0.19 second). And for the full support level case, there was no stress and strain increase during the systolic phase. Moreover, during the diastolic phase, the maximal stress and strain, under all cases, was reduced along with the increase of LVAD support level.

In order to evaluate the biomechanical differences of aortic valve under different support level, the time-average von Mises stress and von Mises strain are illustrated in Figures 4 and 5, respectively. Figure 4 illustrates the distribution of time-average von Mises stress for three leaflets. The range of the von Mises stress was divided into three levels: 0–0.4 MPa, named as low stress level; 0.4–0.8 MPa named as middle stress level; and larger than 0.8 MPa named as high stress level. Figure 4A shows that the time-average von Mises stress in most areas on three leaflets were in the low stress level and middle stress level for all cases studied. And under healthy conditions, the area of low stress level was similar with that of middle stress level (approximate 55% versus 45%). However, the LVAD support level could significantly change this balance. It was seen that along with the increase of support level of LVAD, the area of low stress was gradually reduced, while the area of middle stress was increased accordingly. Once the aortic kept closing during the whole cardiac cycle, the high stress region was observed on the leaflet. In addition, Figure 4B–4F show that the high von Mises stress region was mainly concentrated in the belly and commissure regions.

Figure 5 illustrates the distribution of time-average von Mises strain on three leaflets for all cases. The range of time-average von Mises strain was divided into six levels, in which the width of each level was 0.1. Figure 5A shows that the time-average von Mises strain value on most regions of the leaflets was between 0.1 and 0.2. And the support level of LVAD had little effect. However, when the aortic valve kept closing during the whole cardiac cycle, the time-average von Mises strain value on most regions was increased.

To further evaluate the changes in instantaneous biomechanical states of leaflets, the 3D-distributions of the stress and strain are illustrated in the Figures 6 and 7. Five specified time point (0 seconds, 0.16 seconds, 0.2 seconds, 0.44 seconds, and 0.5 seconds) were chosen to evaluate the changes in the stress and strain during the whole cardiac cycle. Figure 6 illustrated the distribution of stress under all cases during the whole cardiac cycle. It was seen that the distribution of stress was affected by the LVAD support level. The high stress region were

Indexed in: [Current Contents/Clinical Medicine] [SCI Expanded] [ISI Alerting System] [ISI Journals Master List] [Index Medicus/MEDLINE] [EMBASE/Excerpta Medica] [Chemical Abstracts/CAS]

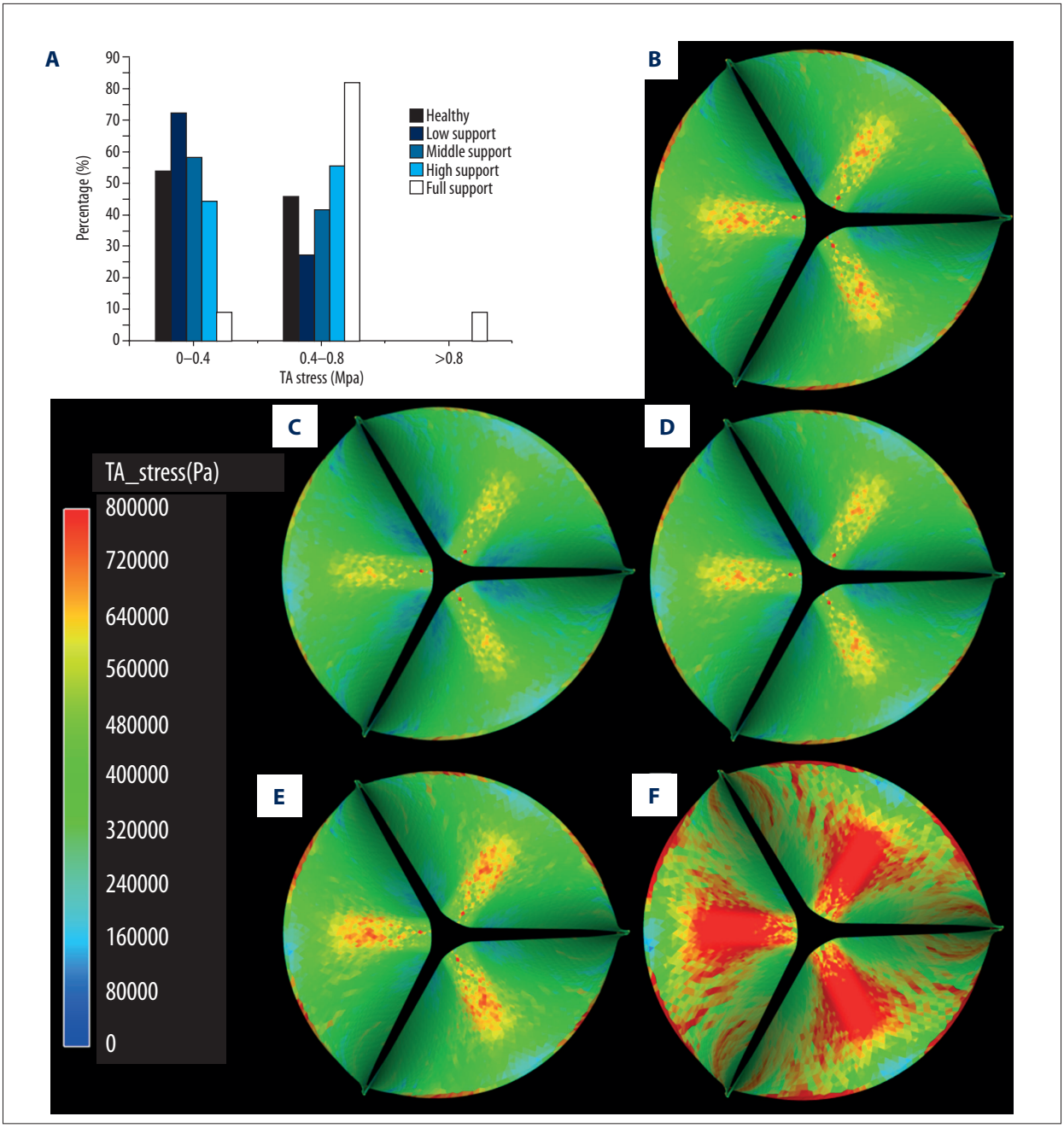

Figure 4. The distribution of time-average von Mises stress. (**A**) The distribution of the time-average von Mises stress in the domain of three leaflets for all cases considered. The width of the bar is 0.4 MPa for time-average von Mises stress. (**B**) The distribution of time-average von Mises stress on the leaflet under healthy condition as the control group. (**C**) The distribution of time-average von Mises stress on the leaflet under low support level case. (**D**) The distribution of time-average von Mises stress on the leaflet under middle support level case. (**E**) The distribution of time-average von Mises stress on the leaflet under high support level case. (**F**) The distribution of time-average von Mises stress on the leaflet under full support level case.

Indexed in: [Current Contents/Clinical Medicine] [SCI Expanded] [ISI Alerting System] [ISI Journals Master List] [Index Medicus/MEDLINE] [EMBASE/Excerpta Medica] [Chemical Abstracts/CAS]

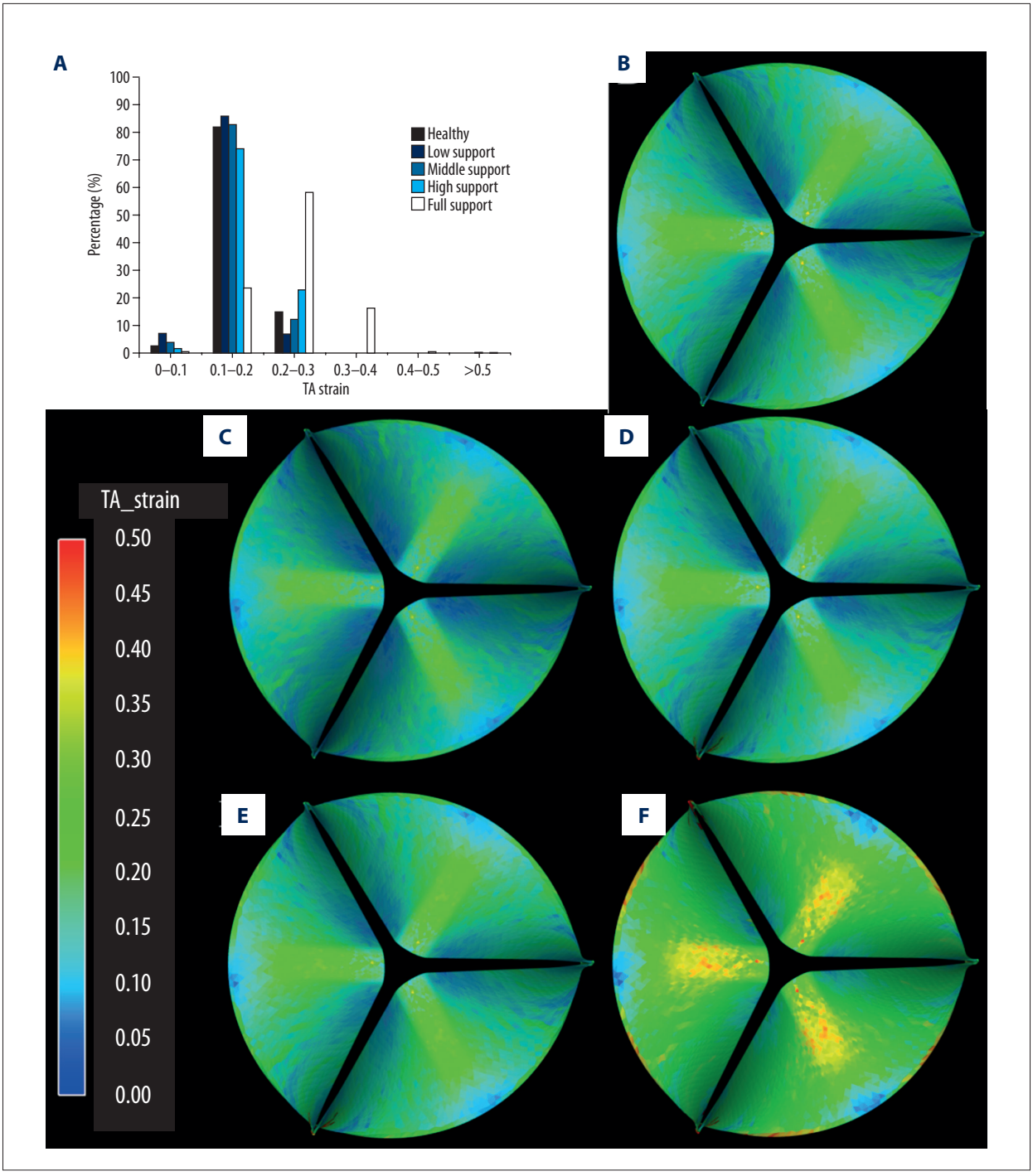

Figure 5. The distribution of time-average von Mises strain. (**A**) The distribution of the time-average von Mises strain in the domain of three leaflets for all cases considered. The width of the bar is 0.1 for time-average von Mises strain. (**B**) The distribution of time-average von Mises strain on the leaflet under healthy condition as the control group. (**C**) The distribution of time-average von Mises strain on the leaflet under low support level case. (**D**) The distribution of time-average von Mises strain on the leaflet under middle support level case. (**E**) The distribution of time-average von Mises strain on the leaflet under high support level case. (**F**) The distribution of time-average von Mises strain on the leaflet under full support level case.

Indexed in: [Current Contents/Clinical Medicine] [SCI Expanded] [ISI Alerting System] [ISI Journals Master List] [Index Medicus/MEDLINE] [EMBASE/Excerpta Medica] [Chemical Abstracts/CAS]

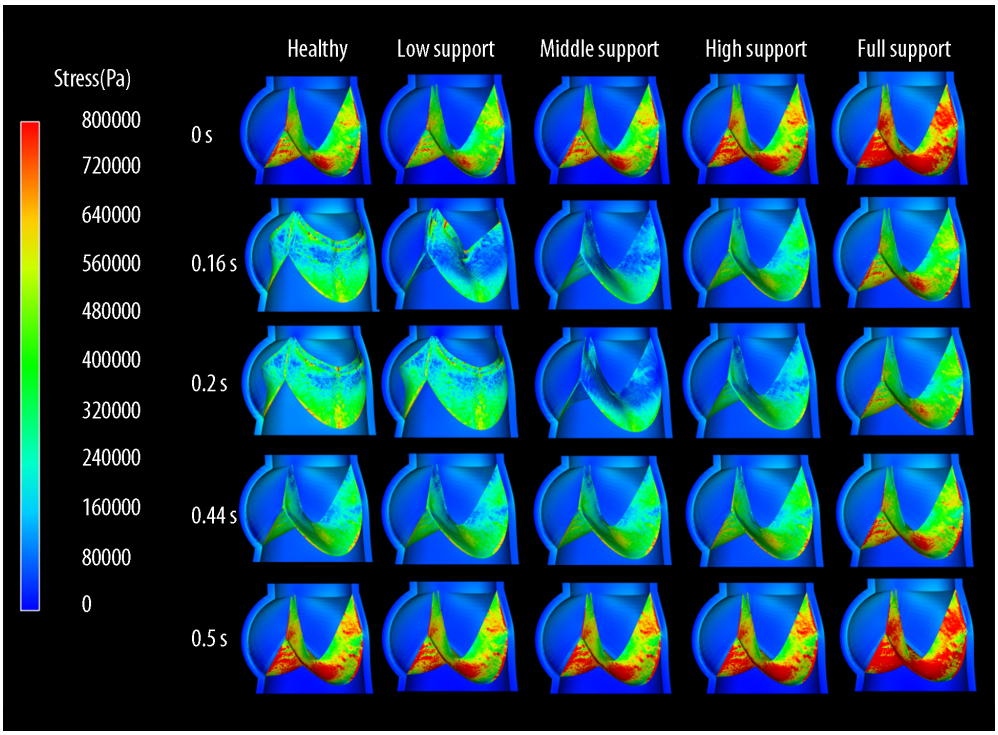

Figure 6. The distribution of the von Mises stress at five specified time point for all cases.

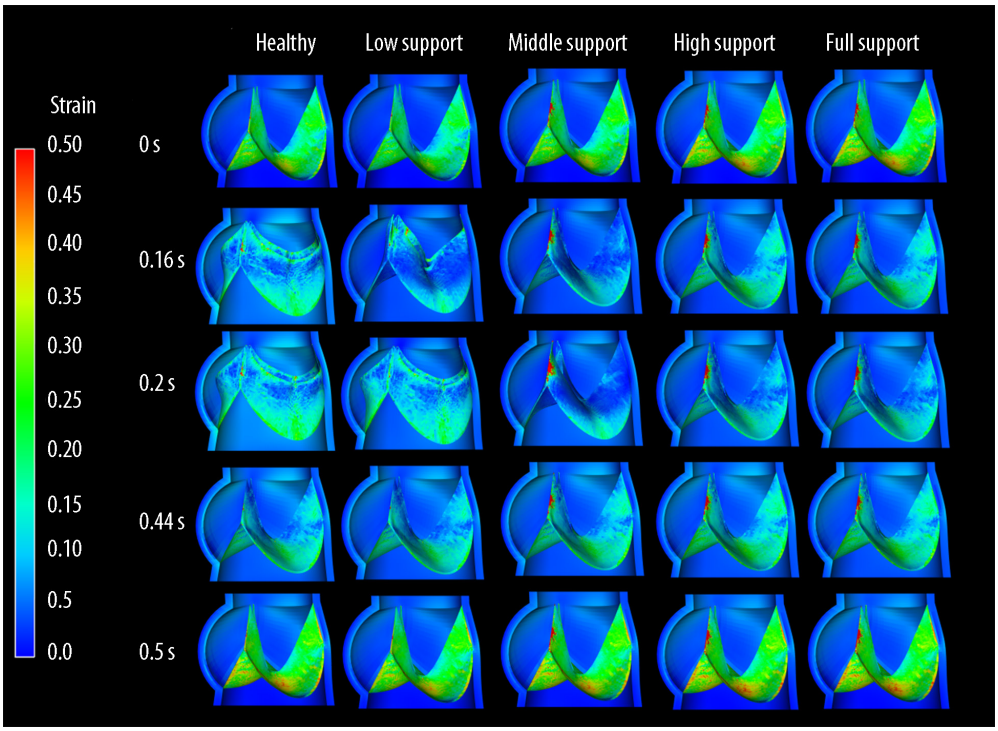

Figure 7. The distribution of the von Mises strain at five specified time point for all cases.

Indexed in: [Current Contents/Clinical Medicine] [SCI Expanded] [ISI Alerting System] [ISI Journals Master List] [Index Medicus/MEDLINE] [EMBASE/Excerpta Medica] [Chemical Abstracts/CAS]

observed at the belly (region a, higher than 1.2 MPa) and commissure (region b, higher than 0.8 MPa) line. During the systolic phase, the value of stress was reduced along with the leaflet opening (region c and d). In contrast, the stress of the leaflet was significantly increased when the leaflet was completely closed at the diastolic phase. And the stress at the attachment line also reached its maximal value during the diastolic phase. Moreover, the area and value of high stress of the aortic leaflet was significantly increased, along with the increase of the LVAD support level. When the leaflet begin to open (at 0.16 seconds), the stress of the leaflet under low support level case, and the stress at the belly which was 0.3 MPa, was significantly lower than that under the other three cases (low support level case 0.3 MPa versus middle support level case 0.48 MPa versus high support level case 0.54 MPa versus full support level case 0.75 MPa). And when the leaflet completely closed at the diastolic phase, the area of stress, at where the stress was higher than 0.8 MPa, under full support level case, was significantly larger than that under the three other cases.

Figure 7 showed the distribution of strain under all cases. It was seen that the strain at the commissure line was significant larger than that at other regions (region a). In addition, the strain of the leaflet was increase along with the increase of LVAD support. At the end diastolic phase (0 seconds), the strain at the belly of the leaflet was increased along with the increase of LVAD support (low support level case 0.3 versus middle support level case 0.35 versus high support level case 0.42 versus full support level case 0.48). In addition, when the aortic valve began to open, the strain of the leaflets were significant reduced. And then, the strain, during diastolic phase, was larger than that during systolic phase. And the strain of leaflet was also increased along with the increase of LVAD support.

A more detailed analysis is shown in Figures 8 and 9, where it was possible to quantify the von Mises stress and von Mises strain percentage distribution on the leaflet at five specified time point. Figure 8 shows that during the systolic phase, the von Mises stress on most of the area (larger than 80%) of the leaflet was in the low stress level (0–0.4 MPa), if the leaflet could open intermittently (Figure 8C, 8D). In contrast, when the aortic valve continuously closed during the whole cardiac cycle, the von Mises stress on most of the area (60%) of the leaflet was in the middle stress level (0.4–0.8 MPa). Moreover, during the diastolic phase, the magnitude of the von Mises stress was significantly increased due to the increase of transvalvular gradients. The magnitude of the von Mises stress on the most of the region (about 75%) of the leaflets was in the middle stress level (0.4–0.8 MPa). And under the full support level case, there was about 40% of the area of the leaflet where the magnitude of the von Mises stress was larger than 0.8 MPa (Figure 8B, 8E, 8F).

Similarly, Figure 9 illustrates the von Mises strain percentage distribution on the leaflet for all cases considered at five specified time point. It was seen that the percentage distribution of von Mises strain was mainly regulated by cardiac phase, rather than the support level of LVAD. During systolic phase, the von Mises strain was mainly less than 0.2. However, during diastolic phase, the von Mises strain was mainly between 0.1–0.4. In contrast, the increase of the support level of LVAD had little effect on the von Mises strain percentage distribution.

Discussion

In this study, FEM studies were conducted to evaluate the effects of LVAD support level on the kinematics and biomechanical states of the aortic valve. Although there have been some studies on the changes in the function and biomechanical states of aortic valve caused by the geometric size [20], the thickness of aortic valve leaflets [21], and the mechanical property of the leaflet [22], there have been no studies on the effects of LVAD support on the aortic valve biomechanical states. The present study is the first study on this topic and provides some useful information to investigators.

Stress has been considered a very important factor, regulating the structure and function of the aortic valve. Xing et al. reported that increases in stress magnitude resulted in significant increases in both collagen and sGAG synthesis [23]. Similarly, Platt et al. found that the valvular cathepsin and MMP activity were seen to be directly regulated by the stress [24]. These changes could result in the alternation of the stiffness of the aortic valve leaflet, and then lead to the occurrence of aortic valve calcification and fusion. In our study, the stress was found to be significantly regulated by the LVAD support level. Along with the increase of the LVAD support level, the area and value of high stress of the leaflet were increased (Figures 4, 6). It is worth noting, that only under the full support level case was the high stress level (larger than 0.8 MPa) observed, which was mainly concentrated at the belly region (Figure 4). This phenomenon may explain why patients that employed the full support strategy have a higher probability of suffering from severe valve fusion [25]. It is likely that the abnormal high stress, observed only in the full support level case, was a key factor for this complication. And the intermittently opening of the aortic valve was confirmed to be a useful method to prevent the valve fusion. Hence, our present study provided the biomechanical evidence to the partial support strategy.

Currently, the strain, as another biomechanical index, is found to have strong mechano-biological effects. For instance, Smith et al. found that cyclic strain reduced expression of pro-inflammatory genes [26]. Gould et al. demonstrated that

Indexed in: [Current Contents/Clinical Medicine] [SCI Expanded] [ISI Alerting System] [ISI Journals Master List] [Index Medicus/MEDLINE] [EMBASE/Excerpta Medica] [Chemical Abstracts/CAS]

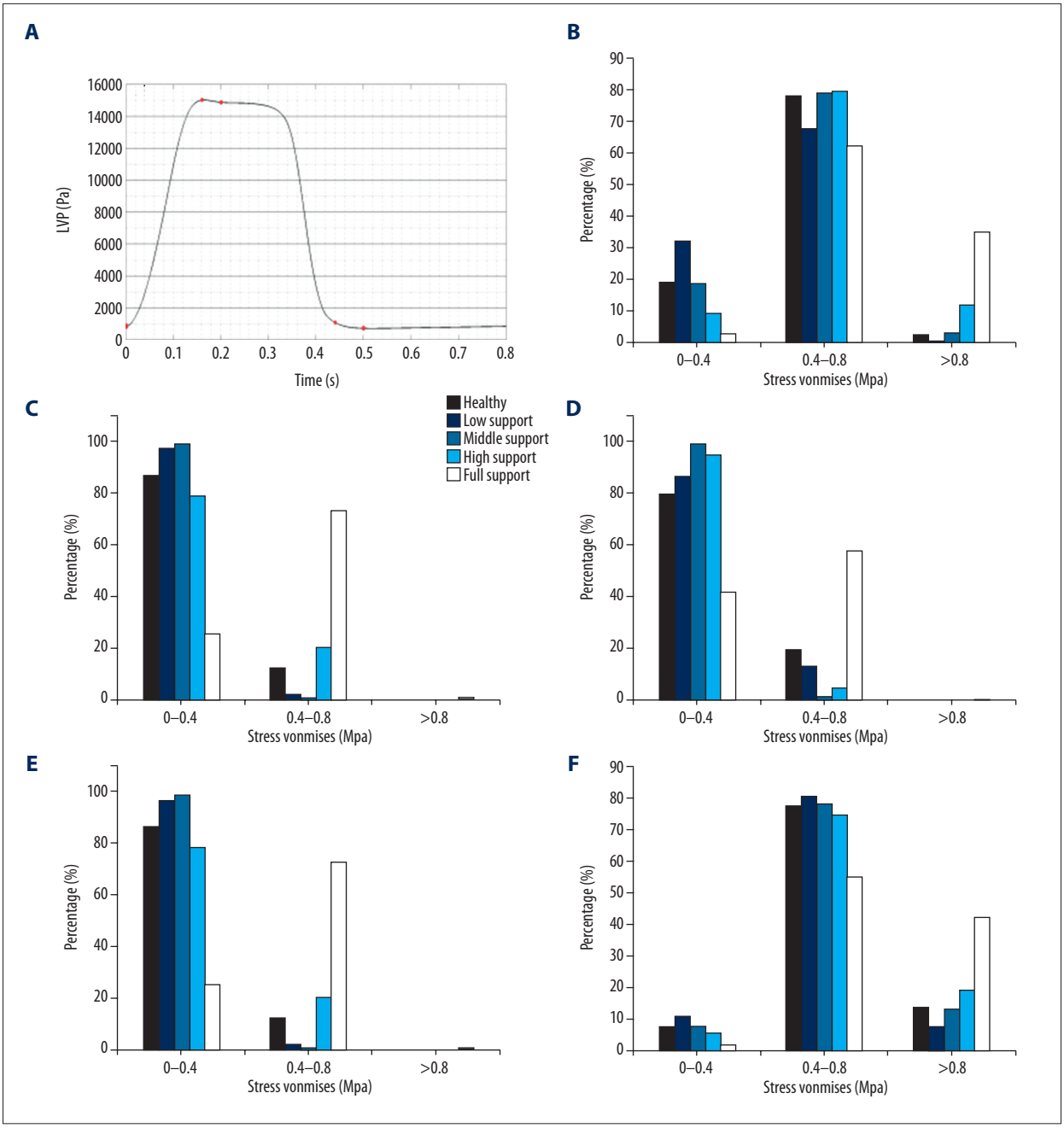

Figure 8. The distribution of von Mises stress in the domain of three leaflets at five specified time point for all cases considered. (**A**) The relationship between the five specified time points (red nodes) and the whole cardiac cycle. (**B**) The distribution of the time-average von Mises stress in the domain of three leaflets at 0 seconds for all cases considered. (**C**) The distribution of the time-average von Mises stress in the domain of three leaflets at 0.16 seconds for all cases considered. (**D**) The distribution of the time-average von Mises stress in the domain of three leaflets at 0.2 seconds for all cases considered. (**E**) The distribution of the time-average von Mises stress in the domain of three leaflets at 0.44 seconds for all cases considered. (**F**) The distribution of the time-average von Mises stress in the domain of three leaflets at 0.5 seconds for all cases considered. The width of the bar is 0.4 MPa for time-average von Mises stress.

Indexed in: [Current Contents/Clinical Medicine] [SCI Expanded] [ISI Alerting System] [ISI Journals Master List] [Index Medicus/MEDLINE] [EMBASE/Excerpta Medica] [Chemical Abstracts/CAS]

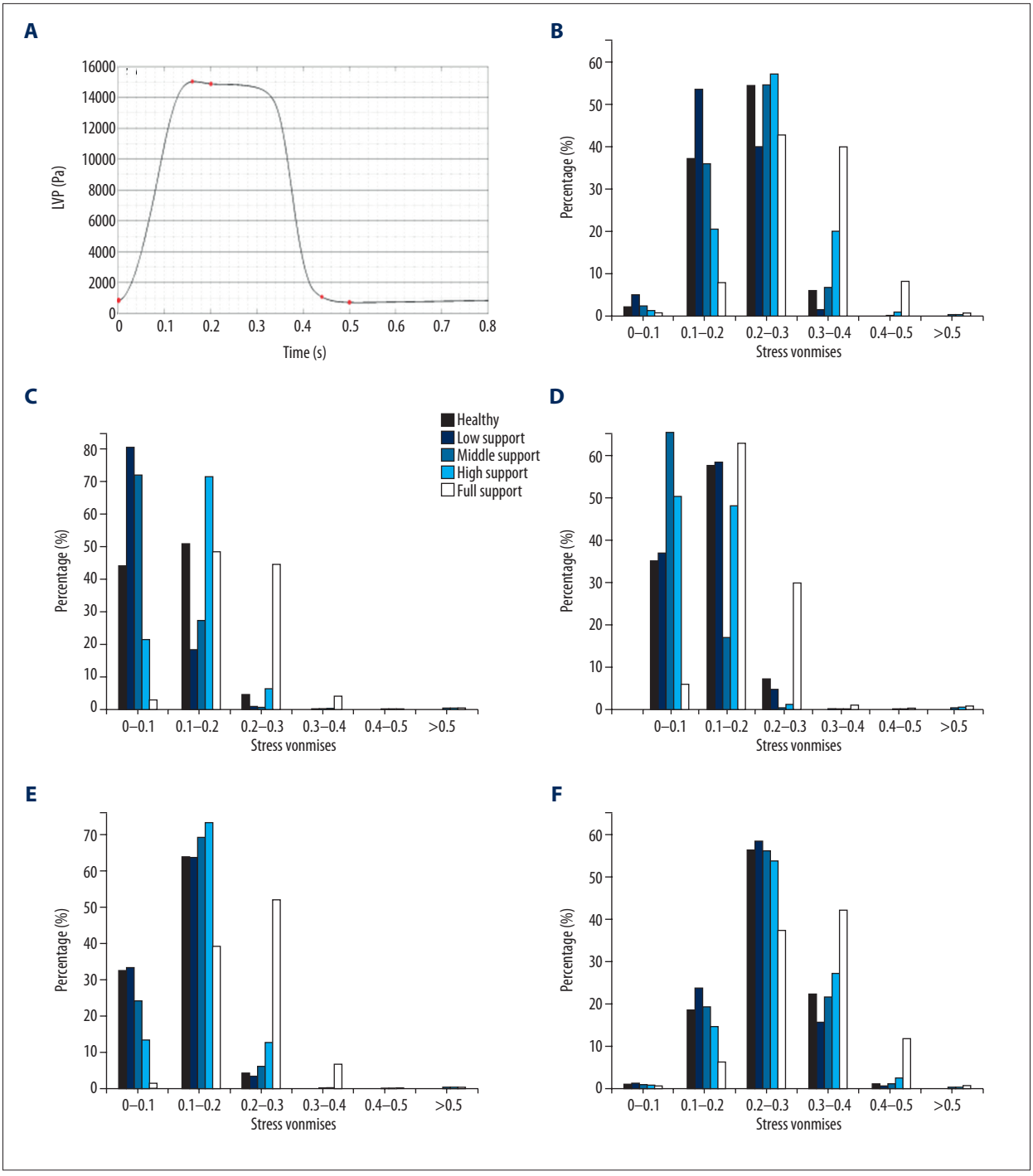

Figure 9. The distribution of von Mises strain in the domain of three leaflets at five specified time point for all cases considered. (**A**) The relationship between the five specified time points (red nodes) and the whole cardiac cycle. (**B**) The distribution of the time-average von Mises strain in the domain of three leaflets at 0 seconds for all cases considered. (**C**) The distribution of the time-average von Mises strain in the domain of three leaflets at 0.16 seconds for all cases considered. (**D**) The distribution of the time-average von Mises strain in the domain of three leaflets at 0.2 seconds for all cases considered. (**E**) The distribution of the time-average von Mises strain in the domain of three leaflets at 0.44 seconds for all cases considered. (**F**) The distribution of the time-average von Mises strain in the domain of three leaflets at 0.5 seconds for all cases considered. The width of the bar is 0.4 MPa for time-average von Mises stress.

Indexed in: [Current Contents/Clinical Medicine] [SCI Expanded] [ISI Alerting System] [ISI Journals Master List] [Index Medicus/MEDLINE] [EMBASE/Excerpta Medica] [Chemical Abstracts/CAS]

the strain field anisotropy was an independent regulator of fibroblast cell phenotype, turnover, and matrix reorganization, which closely regulated the pathological remodeling in aortic valve [27]. Subsequently, Fisher et al. reported that continual exposure to excessive strain accelerated aggregates to calcify into mature nodules that contain a necrotic core surrounded by an apoptotic ring [28]. In our study, the strain of the leaflet was slightly enlarged by increase the LVAD support level, which is consistent with previous study [29] (Figure 5). The high strain regions were observed at the belly and commissure line under both high support level and full support level (Figure 9). Both regions are the high risk region, where calcify was observed in clinical practice. Hence, the results of our study could provide useful information on this area. In addition, previously the support level of LVAD was thought to have a significantly effects on the change in the strain on the leaflet. However, the present study results demonstrated that there was little effect of support level of LVAD on the strain on the leaflet. This may be due to the mechanical property of the leaflet.

Moreover, from these results, it was found that the biomechanical states of leaflets under middle support level case were similar with that under healthy conditions. This was different from previously clinical understandings that the lower the support level of LVAD, the smaller the biomechanical effect on the leaflets. However, the present results demonstrated that there may be an optimal support level, which could achieve the optimal biomechanical states of leaflet. From our present results, we thought that if we kept the duration of aortic valve longer than 0.2 seconds, the LVAD would achieve better performance for maintaining the normal function of aortic valve.

The motion of the aortic valve leaflet under LVAD support is an important question for investigators. Although researchers have demonstrated that LVAD support may reduce the aortic valve ejection duration by *in vitro* experiments, the precise motion of the leaflet under LVAD support has not been measured [30]. In addition, the effect of LVAD support level on the motion of the aortic valve leaflet is also unclear. In this study, the FEM approach was employed to clarify the motion of aortic valve leaflet under different LVAD support levels (Figure 4). It was seen that along with increased LVAD support level, the open duration of the aortic valve was reduced (Figure 4A). Moreover, the maximal radial position (Figure 4A) and radial velocity (Figure 4B) of the aortic valve leaflet was also reduced when the LVAD support level was raised. That means that an increase of LVAD support level would not only reduced the aortic valve area, but also slow down the opening velocity of the aortic valve. These changes may increase the resistance of aortic valve and the left ventricular afterload, which may have the adverse effects on left ventricular function.

Limitation

In this study, an ideal aortic valve model was constructed in which the geometric size of the three leaflets were the same with each other. Although the geometric sizes of the leaflets are different in clinical practice, the geometric model with symmetrical leaflets has been widely used in relative studies. In the future, the patient specific model with asymmetrical leaflets will be used.

In addition, the leaflets were passively driven by blood flow. Hence the FEM study may lose some information on blood flow pattern and shear stress. However, the present study mainly focus on the changes in the stress and strain imposed on the leaflets, hence, neglecting interactions with blood does not affect the assurance of our results. In order to comprehensively study the hemodynamics and biomechanics of the aortic valve, the fluid-structure interaction will be employed in the future.

Conclusions

In this study, the effects of LVAD support level on the motion and biomechanical states of the aortic valve were investigated by using the FEM approach. An ideal aortic valve geometric model was constructed. Four LVAD support levels of LVAD were studied. The results demonstrated that the LVAD support level could significantly change the biomechanical states and the motion of the aortic valve leaflet. Along with the increase of LVAD support level, the RVOT was significant delayed, while the RVCT was not influence. The duration of the ejection and the open area of the aortic valve were also reduced by the increase of LVAD support (low support level case 0.23 seconds versus middle support level case 0.2 seconds versus high support level case 0.14 seconds). Moreover, the area and values of the stress and strain at the leaflet were significant enlarged with the growth of LVAD support level. Along with the increase of the support mode of LVAD, the von Mises stress in most areas of leaflet was increased from the low stress level (0–0.4 MPa) to the middle region (0.4–0.8 MPa). Once the leaflets were continuously closed, the high stress level (larger than 0.8 MPa) was observed. In contrast, the support level of LVAD only had slight effects on the distribution of von Mises strain. According to the aforementioned results, the duration of aortic valve opening larger than 0.2 seconds could achieve better performance of biomechanical states of leaflets.

Indexed in: [Current Contents/Clinical Medicine] [SCI Expanded] [ISI Alerting System] [ISI Journals Master List] [Index Medicus/MEDLINE] [EMBASE/Excerpta Medica] [Chemical Abstracts/CAS]

References:

1. Loebe M, Soltro E, Thohan V et al: New surgical therapies for heart failure. Curr Opin Cardiol, 2003; 18: 194–98
2. Park SJ, Milano CA, Tatooles AG, Rogers JG et al: Outcomes in advanced heart failure patients with left ventricular assist devices for destination therapy. Circ Heart Fail, 2012; 5: 241–48
3. Connelly JH, Abrams J, Klima T et al: Acquired commissural fusion of aortic valves in patients with left ventricular assist devices. J Heart Lung Transplant, 2003; 22: 1291–95
4. Banchs JE, Dawn B, Abdel-Latif A et al: Acquired aortic cusp fusion after chronic left ventricular assist device support. J Am Soc Echocardiogr, 2006; 19: 1401.e1–3
5. Hata H, Fujita T, Ishibashi-Ueda H et al: Pathological analysis of the aortic valve after long-term left ventricular assist device support. Eur J Cardiothorac Surg, 2014; 46: 193–97
6. Butcher JT, Nerem RM: Valvular endothelial cells regulate the phenotype of interstitial cells in co-culture: Effects of steady shear stress. Tissue Eng, 2006; 12: 905–15
7. Butcher JT, Nerem RM: Valvular endothelial cells and the mechanoregulation of valvular pathology. Philos Trans R Soc Lond B Biol Sci, 2007; 362: 1445–57
8. Weston MW, Yoganathan AP: Biosynthetic activity in heart valve leaflets in response to *in vitro* flow environments. Ann Biomed Eng, 2001;29: 752–63
9. Warnock JN, Burgess SC, Shack A, Yoganathan AP: Differential immediate-early gene responses to elevated pressure in porcine aortic valve interstitial cells. J. Heart Valve Dis, 2006; 15: 34–41
10. Balachandran K, Sucosky P, Jo H, Yoganathan AP: Elevated cyclic stretch alters matrix remodeling in aortic valve cusps: Implications for degenerative aortic valve disease. Am J Physiol Heart Circ Physiol, 2009; 296: H756–64
11. Marom G, Halevi R, Haj-Ali R et al: Numerical model of the aortic root and valve: Optimization of graft size and sinotubular junction to annulus ratio. J Thorac Cardiovasc Surg, 2013; 146(5): 1227–31
12. Auricchio F, Conti M, Morganti S et al: Simulation of transcatheter aortic valve implantation: A patient-specific finite element approach. Comput Methods Biomech Biomed Engin, 2014; 17: 1347–57
13. Labrosse MR, Lobo K, Beller CJ: Structural analysis of the natural aortic valve in dynamics: From unpressurized to physiologically loaded. J Biomech, 2010; 43: 1916–22
14. Zhang Y, Gao B, Yu C: The hemodynamic effects of the LVAD outflow cannula location on the thrombi distribution in the aorta: A primary numerical study. Comput Methods Programs Biomed, 2016. 133: 217–27
15. Conti CA, Votta E, Della Corte A et al: Dynamic finite element analysis of the aortic root from MRI-derived parameters. Med Eng Phys, 2010; 32: 212–21
16. Gnyaneshwar R, Kumar RK, Balakrishnan KR: Dynamic analysis of the aortic valve using a finite element model. Ann Thorac Surg, 2002; 73: 1122–29
17. Hallquist JO: LS-DYNA theory manual. In: (LSTC) LSTC. Editor, 2006
18. Cao K, Sucosky P: Computational comparison of regional stress and deformation characteristics in tricuspid and bicuspid aortic valve leaflets. Int J Numer Method Biomed Eng, 2017; 33(3)
19. Sturla F, Votta E, Stevanella M et al: Impact of modeling fluid-structure interaction in the computational analysis of aortic root biomechanics. Med Eng Phys, 2013; 35: 1721–30
20. Marom G, Halevi R, Haj-Ali R et al: Numerical model of the aortic root and valve: Optimization of graft size and sinotubular junction to annulus ratio. J Thorac Cardiovasc Surg, 2013; 146: 1227–31
21. Joda A, Jin Z, Haverich A et al: Multiphysics simulation of the effect of leaflet thickness inhomogeneity and material anisotropy on the stress-strain distribution on the aortic valve. J Biomech, 2016; 49: 2502–12
22. Marom G: Numerical methods for fluid–structure interaction models of aortic valves. Arch Computat Methods Eng, 2015; 22: 595–620
23. Xing Y, Warnock JN, He Z et al: Cyclic pressure affects the biological properties of porcine aortic valve leaflets in a magnitude and frequency dependent manner. Ann Biomed Eng, 2004; 32: 1461–70
24. Platt MO, Xing Y, Jo H et al: Cyclic pressure and shear stress regulate matrix metalloproteinases and cathepsin activity in porcine aortic valves. J Heart Valve Dis, 2006; 15: 622–29
25. John R, Mantz K, Eckman P et al: Aortic valve pathophysiology during left ventricular assist device support. J Heart Lung Transplant, 2010; 29: 1321–29
26. Smith KE, Metzler SA, Warnock JN: Cyclic strain inhibits acute pro-inflammatory gene expression in aortic valve interstitial cells. Biomech Model Mechanobiol, 2010; 9: 117–25
27. Gould RA, Chin K, Santisakultarm TP et al: Cyclic strain anisotropy regulates valvular interstitial cell phenotype and tissue remodeling in three-dimensional culture. Acta Biomater, 2012; 8: 1710–19
28. Fisher CI, Chen J, Merryman WD: Calcific nodule morphogenesis by heart valve interstitial cells is strain dependent. Biomech Model Mechanobiol, 2013; 12: 5–17
29. May-Newman K, Enriquez-Almaguer L, Posuwattanakul P et al: Biomechanics of the aortic valve in the continuous flow VAD-assisted heart. ASAIO J, 2010; 56: 301–8
30. Bozkurt S, van de Vosse FN, Rutten MC: Aortic valve function under support of a left ventricular assist device: continuous *vs.* dynamic speed support. Ann Biomed Eng, 2015; 43: 1727–37

Indexed in: [Current Contents/Clinical Medicine] [SCI Expanded] [ISI Alerting System] [ISI Journals Master List] [Index Medicus/MEDLINE] [EMBASE/Excerpta Medica] [Chemical Abstracts/CAS]